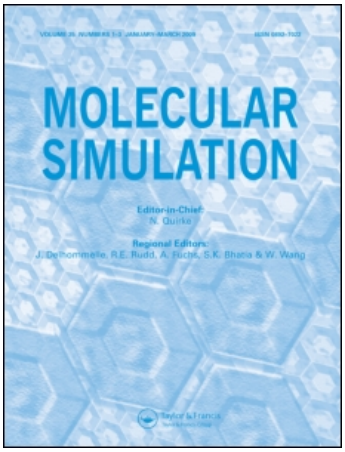

Molecular Simulation
Publication details, including instructions for authors and subscription information:
http://www.informaworld.com/smpp/title~content=t713644482

A GGA+*U* study of the reduction of ceria surfaces and their partial reoxidation through NO_2 adsorption

Natasha M. Galea[a]; David O. Scanlon[a]; Benjamin J. Morgan[a]; Graeme W. Watson[a]
[a] School of Chemistry, Trinity College Dublin, Dublin, Ireland

To cite this Article Galea, Natasha M. , Scanlon, David O. , Morgan, Benjamin J. and Watson, Graeme W.(2009) 'A GGA+*U* study of the reduction of ceria surfaces and their partial reoxidation through NO_2 adsorption', Molecular Simulation, 35: 7, 577 — 583
To link to this Article: DOI: 10.1080/08927020802707001
URL: http://dx.doi.org/10.1080/08927020802707001

Molecular Simulation
Vol. 35, No. 7, June 2009, 577–583

Taylor & Francis
Taylor & Francis Group

A GGA + *U* study of the reduction of ceria surfaces and their partial reoxidation through NO_2 adsorption

Natasha M. Galea, David O. Scanlon, Benjamin J. Morgan and Graeme W. Watson*

School of Chemistry, Trinity College Dublin, Dublin 2, Ireland

(*Received 31 October 2008; final version received 16 December 2008*)

We present the structure and energetics of surface reduction and NO_2 adsorption on the reduced (1 1 1), (1 1 0) and (1 0 0) surfaces of ceria using density functional theory with the generalized gradient approximations (GGA) corrected for on-site Coulomb interactions, GGA + *U*. Vacancy formation at the surfaces of the ceria show reduction of two neighbouring Ce atoms to Ce(III) and gap states in the electronic density of states (EDOS). This gives rise to relaxation of the surface with elongated Ce—O distances around the reduced sites. Reduction is the easiest on the (1 1 0) surface which displays two energetically similar structures with reduction of a sub-surface cerium ion in one of the cases. NO_2 adsorbs strongly on the surface resulting in an asymmetric molecule with significant expansion of the N—O bonds for the oxygen that fills the vacant site. This activation of the molecule is the weakest on the (1 1 0) surface. Analysis of the electronic structure and spin density distributions demonstrates that one Ce(III) has been re-oxidised to Ce(IV), with the formation of an adsorbed NO_2^- species. These results allow a rationalisation of experimental findings and demonstrate the applicability of the GGA + *U* approach to the study of systems in which reduced ceria surfaces play a role.

Keywords: CeO_2; surfaces; GGA + *U*; reduction; NO_2

1. Introduction

Ceria is often used as a promoter or support material in catalysis [1] of both oxidation [2] and reduction [3] reactions. In addition, ceria itself can act as the catalyst in both oxidation and reduction reactions, e.g. in the direct catalytic oxidation of CO and reduction of NO_2 [4]. Ceria's usefulness is based on the ability of cerium to reversibly change oxidation state from Ce(IV) to Ce(III) with the release of oxygen. In Kroger–Vink notation, the surface reduction can be represented as

$$O_o^x + 2Ce_{Ce}^x \rightarrow V_o^{\cdot\cdot} + 2Ce_{Ce}' + \frac{1}{2}O_2 \qquad (1)$$

The oxidation of CO to CO_2 leads to the formation of oxygen vacancies at the surface with reduction of the two neighbouring Ce(IV) atoms to Ce(III). These vacancies are the sites for reduction of NO_2 with the liberated oxygen participating in the surface reoxidation. The use of ceria is therefore based on its ability to store and release oxygen – its oxygen storage capacity (OSC). Given the importance of the OSC of ceria, it is vital to have a comprehensive understanding of this material including the surface reduction and the interaction of reduced surfaces with environmentally sensitive molecules.

The reduction of ceria has been studied using ultraviolet photoemission spectroscopy (UPS) [5] which shows that a localised defect state forms in the middle of the band gap. Previous theoretical studies have shown that density functional theory (GGA-DFT) is not a suitable method for the study of reduced ceria as the resulting electrons are delocalised over all of the Ce atoms in the simulation cell [6–8]. Previous calculations have used the GGA + *U* approach [8,9] or hybrid DFT [10] to correct this delocalisation and have observed reduction of two surface Ce atoms. The reduced Ce atoms are those in the surface layer which were directly coordinated to the removed oxygen.

Experimental studies of the ceria–NO_2 interaction include the interaction of NO_2 with the (1 1 1) surface of ceria on a Pt support [2], NO_2 adsorption onto the ceria (1 1 1) surface [4] and an atomic force microscopy (AFM) study of the interaction of NO_2 with a slightly reduced CeO_2 (1 1 1) surface [11]. UPS [4] and AFM [11] indicate that NO_2 reacts only if the surface is pre-reduced. In this case, NO_2 was found to dissociate into NO, with a corresponding reduction in the intensity of the reduced Ce(III) peak in the UPS spectrum [2,4]. In addition, AFM indicates that the released oxygen was integrated into the surface thus healing the oxygen vacancies. The only calculation to date are those of Nolan et al. [12] using DFT + *U* and the PW91 functional which indicated strong chemisorption on all of the reduced surfaces.

*Corresponding author. Email: watsong@tcd.ie

ISSN 0892-7022 print/ISSN 1029-0435 online

DOI: 10.1080/08927020802707001
http://www.informaworld.com

In this paper, we present a comprehensive study of the reduction and subsequent adsorption of NO_2 on the low index surfaces of ceria.

2. Methods

Our calculations were performed using the VASP package [13,14] in which the valence electronic states are expanded in a basis of plane waves, with the core–valence interaction represented using the projector augmented wave (PAW) approach [15,16]. We use a [He] core for carbon, nitrogen and oxygen and a [Xe] core for cerium. The Perdew–Burke–Ernzerhof (PBE) GGA exchange-correlation functional is applied, as it has replaced the Perdew–Wang (PW91) functional as the standard approach for solid state modelling due to its accuracy and simplicity [17].

Previous studies on ceria surfaces have demonstrated that standard local density approximations (LDA) and generalized gradient approximations (GGA) techniques fail to account for the localised Ce(III) states observed by UPS [5] in reduced ceria [6,8]. The origin of this problem and the self-interaction error (SIE) is due to the approximate exchange found in LDA/GGA DFT which fails to cancel the coulomb self-interaction. We employ the GGA + U methodology of Dudarev [18,19] which penalises partial occupation of the atom-centred orbitals of interest and hence can be used to counter the delocalisation effect caused by the SIE allowing us to describe the highly localised Ce f electronic states. The validity of the GGA + U approach has been demonstrated in its recent use to provide improved descriptions of a wide range of localised electronic defect systems including reduced cations (e.g. reduced TiO_2 [20], Li doped V_2O_5 [21], reduced MoO_3 [22], Fe doped $CoAl_2O_4$ [23]) and oxygen holes (e.g. Al doped SiO_2 [24], Li doped MgO [25]). We have previously discussed the sensitivity of the results to the value of U for GGA + U calculations of ceria [8], and use a $U = 5$ eV for the f orbitals of Ce in all calculations in which Ce ions are present.

The surface is represented in the three-dimensional periodic boundary conditions using the slab model. The two surfaces of the slab are separated in the direction perpendicular to the surface by a vacuum gap of 15 Å. For the (1 1 1) surface a slab 10.5 Å (12 atomic layers) thick is used, for the (1 1 0) surface the slab thickness is 11.5 Å (7 atomic layers), while for the (1 0 0) surface a slab thickness of 10.9 Å (9 atomic layers) is applied. In all cases, a $p(2 \times 2)$ expansion of the surface unit cell is utilised. These expansions of the surface unit cell reduce the defect–defect interactions present in periodic supercell calculations, giving a minimum distance of 7.65 Å between periodic images (on the (1 0 0) surface). The cut-off energy for the plane wave basis is 500 eV, and for sampling the Brillouin zone we use a $4 \times 4 \times 1$ Monkhorst Pack grid, where the last direction is perpendicular to the surface and does not require additional sampling.

For all defective calculations, the O vacancies/NO_2 molecules are present on both sides of the slab so that no net dipole moment is present across the slab. Full geometry relaxation of all surface-adsorbate structures were carried out until the forces were below 0.01 eV Å^{-1}. All calculations were spin polarised with the spin degrees of freedom allowed to relax. In cases where there was more than one Ce(III) ions present, both ferromagnetic and anti-ferromagnetic configurations are possible and found to be of almost identical energy and hence we report the results from the ferromagnetic solutions. Molecular calculations used for comparison with the adsorbed systems were carried out in 10 Å cube cell, using the same exchange-correlation functional and plane wave cut-off, with sampling at the Γ-point. The vacancy formation energy is given by

$$E_{\text{ads}} = 0.5([E(CeO_2[2Vac]) + E(O_2)] - E(CeO_2)), \quad (2)$$

where $E(CeO_2[2Vac])$ is the energy of the reduced slab with one oxygen vacancy on each side of the slab, $E(CeO_2)$ is the energy of the stoichiometric slab and $E(O_2)$ is the energy of an O_2 molecule. The energy of the O_2 molecule is taken from DFT calculations, although it is known that PBE DFT overestimates the binding energy of O_2 by approximately 1.4 eV [26]. The results presented here have not been adjusted for this error.

The NO_2 adsorption energy per molecule is calculated from

$$E_{\text{ads}} = 0.5(E(CeO_2[2Vac]\_2(NO_2)_{\text{ads}}) - [E(CeO_2[2Vac]) + 2^* E(NO_2)]), \quad (3)$$

where $E(CeO_2[2Vac]\_2(NO_2)_{\text{ads}})$ is energy of the simulation cell containing the reduced surface with two adsorbate molecules, one on each surface, and $E(NO_2)$ is the energy of a single molecule in the gas phase. Negative adsorption energies signify that the adsorption structure is stabilised compared with the initially isolated species.

3. Reduction of ceria surfaces

For the (1 1 1) surface all of the surface oxygen atoms are equivalent and are coordinated to three Ce atoms (see Figure 1(a) generated using the VESTA package [27]). On removal of one oxygen atom, there are three possible equivalent Ce atoms that can be reduced. Relaxation of the surface results in two of these having long Ce—O_{surf} distances from 2.45 to 2.46 Å. The third Ce atom (Ce3) has much smaller Ce—O_{surf} bond lengths of 2.30 and 2.31 Å.

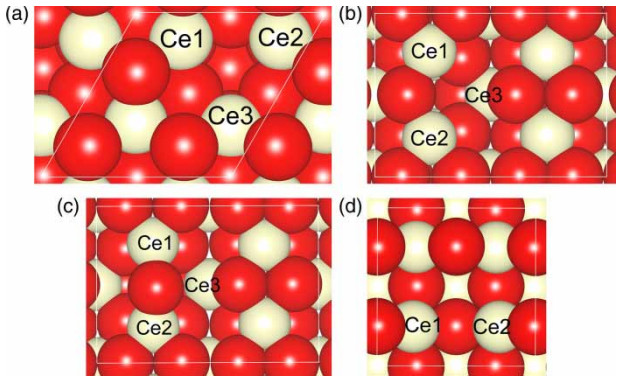

Figure 1. Plan view of the relaxed structure of the reduced (a) (1 1 1) surface, (b) (1 1 0) surface and (c) split vacancy (1 1 0) surface and (d) the (1 0 0) surface.

The (1 1 0) surface has a structure in which there are two oxygen rows with a row of Ce atoms between them (Figure 1(b)). There is only one unique oxygen site on the (1 1 0) surface but relaxation of this can achieve two different structural geometries. The vacancy can relax locally forming the simple vacancy structure in Figure 1(b) resulting in significant distortion around the two surface Ce atoms originally coordinated to the removed oxygen. The two Ce atoms in the surface layer (Ce1 and Ce2) are equivalent with surface Ce—O distances of 2.33, 2.27 and 2.36 Å compared with 2.34 Å in the pure surface. The nearest neighbour subsurface Ce3 shows less distortion and relaxes away from the vacancy giving rise to slightly reduced Ce—O distances (average 2.32 Å) compared to the pure surface.

An alternative conformation (Figure 1(c)) occurs when the oxygen in the next row which is coordinated to the same Ce atoms as the removed oxygen takes up a position almost equidistance between the vacancy site and its original lattice site (a split vacancy). It bridges the two Ce atoms in the Ce row and relaxes out of the surface to allow lengthening of the Ce—O distances. However, the Ce—O distances are not symmetric with a particularly short Ce2—O, 2.09 Å, compared with the Ce1—O distance of 2.32 Å. The average Ce—O distance is much shorter around Ce2 (average of 2.17 Å) than Ce1 (average of 2.34 Å). The Ce3—O distances are also different showing significant expansion of the distances to the nearest oxygen atoms for the split vacancy with an average Ce3—O distance of 2.43 Å.

For the (1 0 0) surface the oxygen atoms are all equivalent and two coordinate. On the removal of one oxygen atom the two nearest neighbour cerium atoms relax equivalently (Figure 1(d)) with the one remaining Ce—O_{surf} distance of 2.18 Å compared with the stoichiometric surface distance of 2.19 Å. The remaining four Ce—O distances for Ce1 and Ce2 range from 2.37 to 2.55 Å.

Vacancy formation on the (1 1 1) surface is least favourable, at 2.57 eV, which is expected due to the compact nature of the surface and the low surface energy [8]. For the (1 1 0) surface, the distorted structure with the split vacancy is slightly more stable with a formation energy of 1.61 eV compared to the simple vacancy structure previously observed [8,9,28] with a formation energy of 1.66 eV. It should be noted that although the energy for the simple vacancy in the present study is less favourable than the split vacancy, it is considerably more stable than that previously reported (e.g. 1.99 eV [8,28]). Test calculations have shown that this is due to the smaller $p(2 \times 1)$ unit cell utilised in previous studies which overestimates the formation energy of the vacancy. Our results are similar to those of Fabris et al. [9] who also used a $p(2 \times 2)$ cell. For the (1 0 0) surface the vacancy formation energy is 2.17 eV, despite it being the least stable surface [8]

All of the reduced surfaces give rise to similar electronic density of states (EDOS) to that of the (1 1 1) surface shown in Figure 2. In all cases, a filled gap state has appeared in the middle of the band gap that from projection onto spherical harmonics can be shown to be composed of Ce 4*f* states. Integration of the peak shows two electrons per oxygen vacancy and the partial charge density for this peak shows that two cerium atoms have been reduced in each case (Figure 3). For the (1 1 1) surface, this reduction (Figure 3(a)) shows that the two equivalent Ce atoms with longer Ce—O bonds have been reduced to Ce(III) while the third Ce atom remains Ce(IV). For the (1 1 0) surface the simple vacancy, as previously reported, shows reduction of the surface atoms (Figure 3(b)). However, the split vacancy shows reduction of one surface atom and the nearest neighbour sub surface Ce3 atom (Figure 3(c)). The reduction of one of the two initially equivalent surface Ce atoms is the reason for the asymmetry in the split

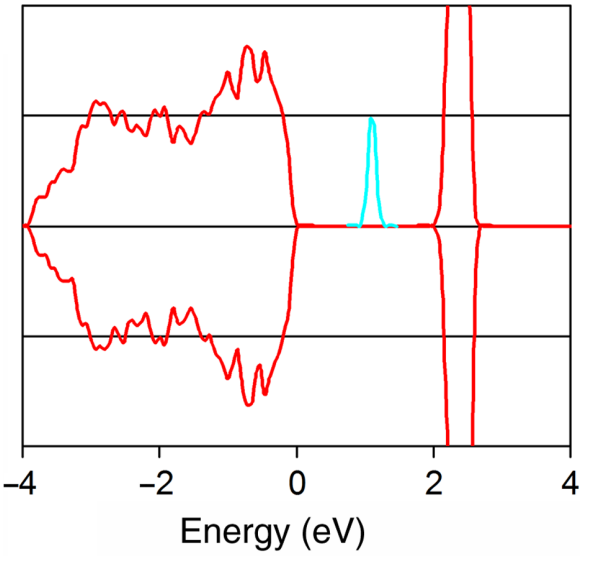

Figure 2. Total electronic density of states for the reduced (1 1 1) surface of ceria with the top of the valence band set to 0 eV.

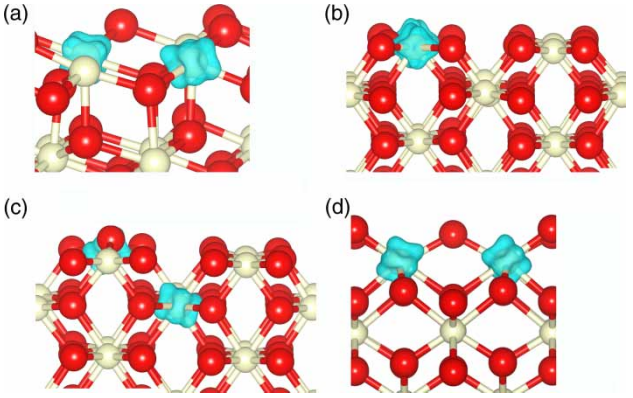

Figure 3. Partial charge densities of the gap state in the reduced (a) (1 1 1), (b) (1 1 0), (c) split vacancy (1 1 0) and (d) (1 0 0) surface of ceria at a contour level of 0.1 e Å^{-3}.

vacancy (1 1 0) surface structure. For the (1 0 0) surface there are only two adjacent surface Ce atoms and these have both been reduced (Figure 3(d)).

4. Adsorption of NO_2 on reduced ceria surfaces

The relaxed geometries of NO_2 adsorbed onto the three reduced ceria surfaces are shown in Figure 4 (adsorption on the simple and split vacancy of the (1 1 0) surface gives rise to the same result). For ease of discussion, the two reduced Ce(III) ions of the initial reduced surface are indicated by the green (Ce1) and the yellow (Ce2) spheres to facilitate discussion of the change in the geometry and electronic structure of the surface. The NO_2 molecule adsorbs onto the surface through one of the oxygen atoms, which occupies the vacancy site. The molecule displays a bent configuration with the remaining N—O bond pointing towards the Ce1 atom. The oxygen atom of the NO_2 molecule that sits at the vacancy site is denoted O_V while the other oxygen atom of NO_2 will be denoted O_N.

The adsorption is strongly exothermic on all reduced surfaces with adsorption energies of −2.30 eV for the (1 1 1) surface, −1.98 eV for the (1 1 0) surface and −2.28 eV for the (1 0 0) surface. This indicates a strong interaction between the molecule and the reduced oxide surface.

Adsorption of NO_2 on the surfaces results in significant elongation of the N—O_V bond length from its gas phase value of 1.21 to 1.35 Å on the (1 1 1) surface, 1.30 Å on the (1 1 0) surface and 1.36 Å on the (1 0 0) surface. The N—O_N distance changes only slightly to 1.23, 1.26 and 1.23 Å on the (1 1 1), (1 1 0) and (1 0 0) surfaces, respectively. This data indicate that although there is significant lengthening of the N—O_V bond, it is clear that dissociation to NO and a lattice oxygen is not observed, indicating that there is an energy barrier to the breaking of this bond. This is in line with the experimental observation that a temperature of 300 K is required for the dissociation of NO_2 on reduced ceria [4]. It is also clear from this that the (1 1 0) surface does not activate the molecule to the same extent as the other surfaces.

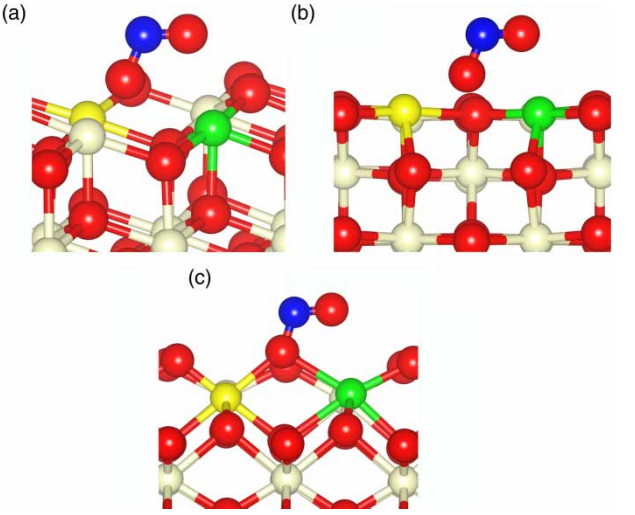

Figure 4. Structure of NO_2 adsorbed onto the reduced (a) (1 1 1) surface, (b) (1 1 0) surface and (c) (1 0 0) surface of ceria.

Adsorption of NO_2 onto the reduced (1 1 1) surface results in an asymmetric environment (Figure 4(a)) with the Ce—O_V distances of 2.81 and 2.69 Å for Ce1 and Ce2, respectively (see Table 1). The third previously unreduced Ce has a Ce—O_V distance of 2.62 Å indicating that all three Ce atoms are inequivalent. These distances are significantly longer than the Ce(IV)—O distances of the stoichiometric surface (2.37 Å) or the Ce(IV)—O and Ce(III)—O distances of the reduced surface (2.30 and 2.46, respectively). The O_N atom is coordinated to Ce1 with a longer distance of 2.74 Å. When NO_2 is adsorbed onto the reduced (1 1 0) surface, O_V is closer to Ce2 than Ce1, with Ce—O_V distances of 2.87 Å (Ce1) and 2.60 Å (Ce2) (Figure 4(b)). These are considerably longer than the stoichiometric surface and result in the molecule being considerably above the surface plane. This is in line with the weaker interaction and smaller activation of the molecule on this surface. The resulting Ce1—O_N distance is shorter (2.61 Å) than on the (1 1 1) surface due to the cations being in the same plane as the anions on the (1 1 0) surface. Upon adsorption of NO_2 on the reduced (1 0 0) surface, the Ce—O_V distances are 2.65 Å for Ce1 and 2.40 Å for Ce2 which are significantly shorter than on the other surfaces. Indeed, it is clear from Figure 4(c), that the O_V oxygen occupies a position much closer to the oxygen lattice site than on the other two surfaces. With a corrugated surface structure, it is much more difficult for the O_N to interact with the surface Ce atoms resulting in a long Ce1—O_N distance of 2.84 Å.

The general features of the EDOS for NO_2 adsorption are similar for all three surfaces, and we will only display the total EDOS for the (1 1 1)-NO_2 surface-adsorbate

Table 1. Adsorption energy and molecular structural data for the reduced surface and NO_2 adsorbed onto the reduced surfaces.

	(1 1 1)	(1 1 0)	(1 0 0)	NO_2	NO_2^-
NO_2 adsorption energy (eV)	−2.27	−1.61	−2.28	–	–
O_V formation energy (eV)	2.57	1.66	2.17	–	–
N—O_V distance (Å)	1.36	1.30	1.35	1.21	1.26
N—O_N distance (Å)	1.23	1.26	1.23	1.21	1.26
Ce1—O_V (Å)	2.81	2.87	2.65	–	–
Ce2—O_V (Å)	2.69	2.60	2.40	–	–
Ce1—O_N (Å)	2.74	2.61	2.84	–	–

structure (Figure 5). In the total EDOS, we find a standard EDOS as expected for ceria with the addition of a small narrow peak lying between the top of the valence band and the bottom of the unoccupied Ce 4*f* derived peak. This is due to the presence of reduced ceria as observed in the vacancy calculations. However, if we integrate the band gap peak, we find one electron per surface rather than the two electrons of the reduced surface indicating that the surfaces have been partially oxidised.

To examine the surface oxidation, we plot the excess spin density for all three surfaces in Figure 6. This shows that a *single* reduced Ce(III) ion remains on the surfaces, the other having been re-oxidised to Ce(IV). However, unlike the reduced surfaces, the location of the Ce(III) does not correlate with the structure. As can be seen in Figure 6 the spin density associated with the Ce(III) is not always associated with the elongated Ce—O_V bonds (Ce1 – green atoms). For both the (1 1 1) and the (1 1 0) surface the Ce(III) site has the shorter bond (Ce2). This is contrary to previously published results [12], where the Ce(III) ion was always associated with the long Ce—O_V distance. Additional calculations were performed with a distorted structure to encourage the localisation of the charge onto the Ce1 site for the (1 1 1) and (1 1 0) surfaces and onto the Ce2 site for the (1 0 0) surfaces. This was successful and the site maintained similar elongated bonds and structure despite the electronic rearrangement. The energies show that we had indeed initially found the most stable electronic configuration and that the Ce(III) on site Ce1 was less stable by 0.03 and 0.14 eV, respectively, for the (1 1 1) and (1 1 0) surfaces and more stable by 0.07 eV for the (1 0 0) surface. A further calculation in which the NO_2 was rotated confirmed that the elongated bond was associated with the interaction of both of the NO_2 oxygen atoms with Ce sites. The steric constraint of getting both oxygen atoms to interact is the cause of the elongation of the bond and overrides the size of the Ce(III) ion. The different structure and ensuing electric field result in the variation with surface structure of the location of the most stable Ce(III) site.

NO_2 is a radical, and since there is no suggestion of spin density on the molecule in Figure 6, we can surmise that the missing surface electron has been transferred to the molecule forming NO_2^-. To confirm the nature of the adsorbed NO_2, we have analysed the charge density and partial electronic density of states (PEDOS). Partial atomic

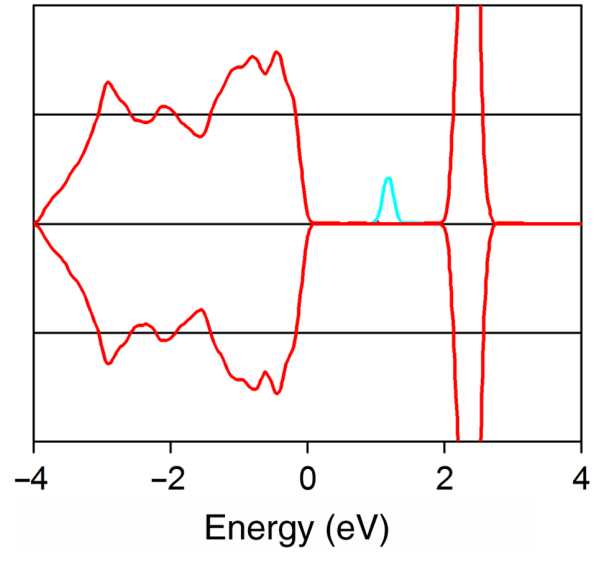

Figure 5. Total electronic density of states for the NO_2-(1 1 1) ceria surface. The top of the valence band has been set to 0 eV.

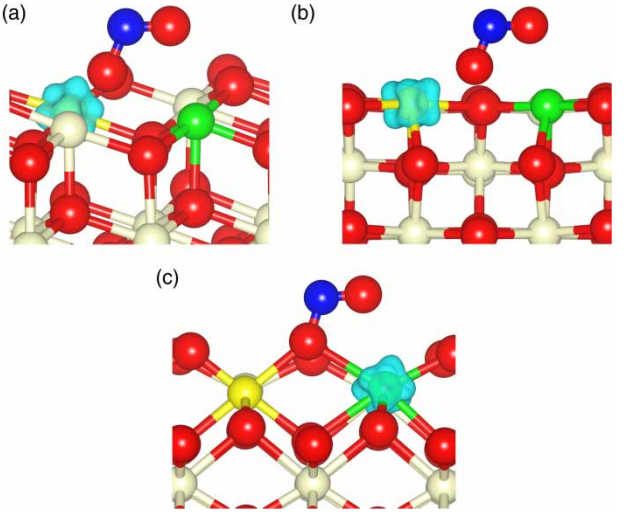

Figure 6. Spin density (0.1 e Å^{-3}) resulting from NO_2 adsorption onto the (a) (1 1 1) surface, (b) the (1 1 0) surface and (c) the (1 0 0) ceria surface.

charges, derived from Bader analysis [29], show that the total charge on adsorbed NO_2 has increased between 0.7 and 0.9 electrons. In addition, the observed lengthening of the N—O bonds upon adsorption further supports the presence of an anionic NO_2^- species. Symmetric elongation of the N—O bond distances from 1.21 to 1.26 Å is seen in gas phase NO_2^-, with the asymmetric bond elongation found in the adsorbed species due to the asymmetric electric field present at the surface as well as activation of the molecule towards N—O bond cleavage. The PEDOS for the N 2*p* and O 2*p* of gas phase NO_2, NO_2 adsorbed on the (1 1 1) surface and gas phase NO_2^- are shown in Figure 7. Gas phase NO_2 has an open shell character as expected, while spin pairing is observed for the adsorbed species. A similar spin pairing and composition of the states is present for the NO_2^- anion

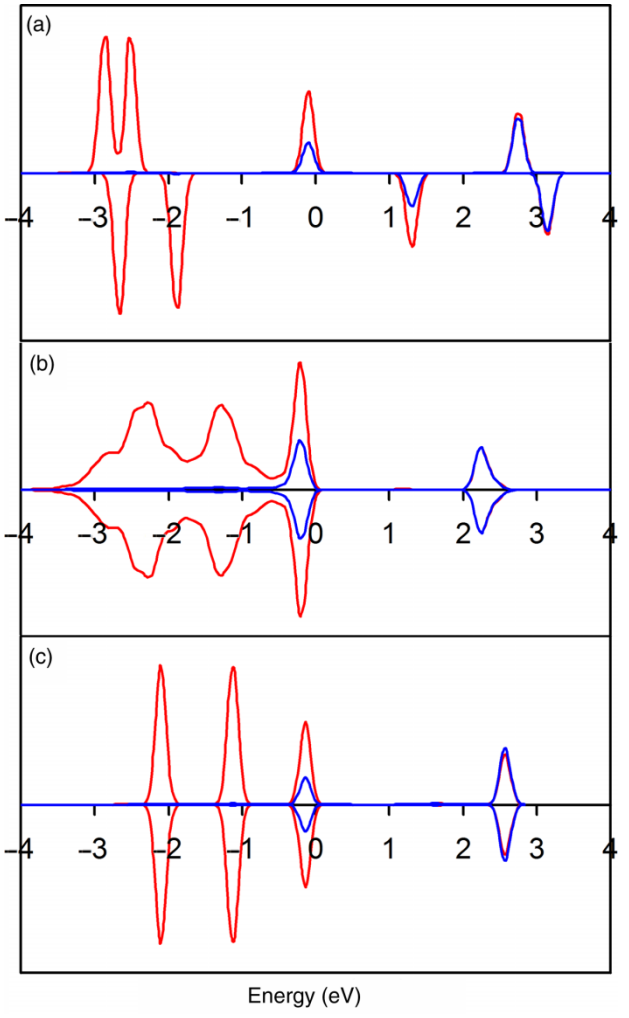

Figure 7. Partial electronic density of states showing the oxygen *p* states (red, or grey while viewed in mono) and nitrogen *p* states (blue, or black while viewed in mono) for (a) gas phase NO_2, (b) NO_2 adsorbed on the (1 1 1) surface of ceria and (c) gas phase NO_2^- molecule. The top of the valence band has been set to 0 eV.

confirming that the adsorbed NO_2 has received an electron from the surface forming adsorbed NO_2^-.

5. Discussion

Table 1 summarises some of the data for the reduced and NO_2 adsorbed systems. For surface reduction, we find the (1 1 0) surface is significantly easier to reduce. Indeed, our reduction energy is considerably smaller than that previously reported by Nolan et al. (1.99 eV) which we can attribute to our larger $p(2 \times 2)$ surface. The formation of the oxygen vacancy is more favourable on the $p(2 \times 2)$ slab than the $p(2 \times 1)$ slab used by Nolan et al. [8] which also has implications for the NO_2 adsorption on this surface as the reduced surface is the starting point for NO_2 adsorption. From Table 1, it can be seen that the NO_2 adsorption energy is closely linked to the vacancy formation energy. Given that our analysis shows that the adsorption of NO_2 can be viewed as a partial healing of the vacancy both geometrically, with the NO_2 occupying the vacant site, and electronically, with partial reoxidation of the surface, this should not be unexpected. The link between the vacancy formation and NO_2 adsorption appears to impact on the degree of activation of the NO_2 molecule. The (1 1 0) surface shows the easiest vacancy formation and hence the lowest adsorption energy for NO_2. This weaker interaction results in a significantly different molecular structure to the other surfaces. In Table 1, the N—O_V bond distances show that the elongation and hence the activation of the molecule is significantly smaller for the (1 1 0) surfaces. Since this is the bond that must break to heal the surface and release NO, this is likely to have a significant impact on the activity of deNO_x catalysis on this surface.

6. Conclusions

In order to contribute to the understanding of catalysis at the surfaces of ceria, we have investigated the reduction of ceria surfaces and their subsequent interaction with NO_2 using the GGA + *U* approach.

Surface reduction shows that on the loss of an oxygen atom two Ce atoms are reduced to Ce(III). This reduction gives rise to the characteristic band gap peaks in the EDOS. The reduction is the easiest on the (1 1 0) surface, where two different structures and Ce(III) locations were observed. One of these, the split vacancy, displays for the first time sub-surface reduction and this was found to be slightly more stable than the previously reported surface reduction. The (1 0 0) shows the next easiest reduction with the electrons localised on the two nearest neighbour Ce atoms to the vacancy. The (1 1 1) surface has three coordinate oxygen and hence on reduction two of the three equivalent Ce atoms are reduced breaking the surface symmetry. Owing to the low surface energy and compact structure, the (1 1 1) surface is the hardest to reduce.

The adsorption of NO_2 on the reduced surfaces is highly exothermic with energy gains of at least 2.25 eV, the most favourable being the (1 1 1) surface that can be attributed to the healing of the oxygen vacancy which is least favourable on the (1 1 1) surface. For all the surfaces, we observe partial reoxidation of the Ce^{3+} ions with one electron being transferred from one of the Ce(III) sites on the surface to the NO_2 molecule to form NO_2^- as an intermediate adsorption structure. Lengthening of one N—O bond by around 10% is found, which is a necessary step in the formation of free NO and full reoxidation of the surface. The electron transfer and reoxidation is confirmed by analysis of the electronic structure.

We have demonstrated that the GGA + *U* approach can provide a description of reduced ceria and of the adsorption of molecules on ceria surfaces which is consistent with experimental findings and advances our understanding of the processes involved in ceria based catalysis.

Acknowledgements

This material is based upon works partially supported by the Science Foundation Ireland under Grant Numbers 04/BR/C0216 and 06/IN.1/I92. We also acknowledge the EPSRC for funding of and access to the Mott2 computer, under grant GR/S84415/01 and the HEA and NDP for the PRTLI programmes IITAC and e-INIS and the Trinity Centre for High Performance Computing for access to the TCHPC computational facilities.

References

[1] A. Trovarelli, *Catalysis by Ceria and Related Materials*, Imperial College Press, London, 2002, pp. 343–376.

[2] U. Berner, K. Schierbaum, G. Jones, P. Wincott, S. Haq, and G. Thornton, *Ultrathin ordered CeO_2 overlayers on Pt(1 1 1): interaction with NO_2, NO, H_2O and CO*, Surf. Sci. 467 (2000), pp. 201–213.

[3] D.R. Mullins and S.H. Overbury, *Coverage dependent dissociation of NO on Rh supported on cerium oxide thin films*, Surf. Sci. 511 (2002), pp. L293–L297.

[4] J.A. Rodriguez, T. Jirsak, S. Sambasivan, D. Fischer, and A. Maiti, *Chemistry of NO_2 on CeO_2 and MgO: experimental and theoretical studies on the formation of NO_3*, J. Chem. Phys. 112 (2000), pp. 9929–9939.

[5] M.A. Henderson, C.L. Perkins, M.H. Engelhard, S. Thevuthasan, and C.H.F. Peden, *Redox properties of water on the oxidized and reduced surfaces of CeO_2 (1 1 1)*, Surf. Sci. 526 (2003), pp. 1–18.

[6] M. Nolan, S. Grigoleit, D.C. Sayle, S.C. Parker, and G.W. Watson, *Density functional theory studies of the structure and electronic structure of pure and defective low index surfaces of ceria*, Surf. Sci. 576 (2005), pp. 217–229.

[7] S. Fabris, S. de Gironcoli, S. Baroni, G. Vicario, and G. Balducci, *Taming multiple valency with density functionals: a case study of defective ceria*, Phys. Rev. B 71 (2005), 041102.

[8] M. Nolan, S.C. Parker, and G.W. Watson, *The electronic structure of oxygen vacancy defects at the low index surfaces of ceria*, Surf. Sci. 595 (2005), pp. 223–232.

[9] S. Fabris, G. Vicario, G. Balducci, S. de Gironcoli, and S. Baroni, *Electronic and atomistic structures of clean and reduced ceria surfaces*, J. Phys. Chem. B 109 (2005), pp. 22860–22867.

[10] J.L.F. Da Silva, M.V. Ganduglia-Pirovano, J. Sauer, V. Bayer, and G. Kresse, *Hybrid functionals applied to rare-earth oxides: the example of ceria*, Phys. Rev. B 75 (2007), 045121.

[11] Y. Namai, K. Fukui, and Y. Iwasawa, *The dynamic behaviour of CH_3OH and NO_2 adsorbed on CeO_2 (1 1 1) studied by noncontact atomic force microscopy*, Nanotechnology 15 (2004), pp. S49–S54.

[12] M. Nolan, S.C. Parker, and G.W. Watson, *Reduction of NO_2 on ceria surfaces*, J. Phys. Chem. B 110 (2006), pp. 2256–2262.

[13] G. Kresse and J. Hafner, Ab initio *molecular-dynamics simulation of the liquid-metal–amorphous semiconductor transition in germanium*, Phys. Rev. B 49 (1994), pp. 14251–14269.

[14] G. Kresse and J. Furthmuller, *Efficiency of* ab initio *total energy calculations for metals and semiconductors using a plane-wave basis set*, Comp. Mat. Sci. 6 (1996), pp. 15–50.

[15] P.E. Blöchl, *Projector augmented-wave method*, Phys. Rev. B 50 (1994), pp. 17953–17979.

[16] G. Kresse and D. Joubert, *From ultrasoft pseudopotentials to the projector augmented-wave method*, Phys. Rev. B 59 (1999), pp. 1758–1775.

[17] J.P. Perdew, K. Burke, and M. Ernzerhof, *Generalized gradient approximation made simple*, Phys. Rev. Lett. 77 (1996), pp. 3865–3868.

[18] V.I. Anisimov, J. Zaanen, and O.K. Andersen, *Band theory and Mott insulators: Hubbard U instead of Stoner I*, Phys. Rev. B 44 (1991), pp. 943–954.

[19] S.L. Dudarev, G.A. Botton, S.Y. Savrasov, C.J. Humphreys, and A.P. Sutton, *Electron-energy-loss spectra and the structural stability of nickel oxide: an LSDA+U study*, Phys. Rev. B 57 (1998), pp. 1505–1509.

[20] B.J. Morgan and G.W. Watson, *A DFT + U description of oxygen vacancies at the TiO_2 rutile (1 1 0) surface*, Surf. Sci. 601 (2007), pp. 5034–5041.

[21] D.O. Scanlon, A. Walsh, B.J. Morgan, and G.W. Watson, *An* ab initio *study of the reduction of V_2O_5 through the formation of oxygen vacancies and Li intercalation*, J. Phys. Chem. C 112 (2008), pp. 9903–9911.

[22] R. Coquet and D.J. Willock, *The (0 1 0) surface of α-MoO_3, a DFT + U study*, Phys. Chem. Chem. Phys. 7 (2005), pp. 3819–3828.

[23] A. Walsh, Y. Yan, M.M. Al-Jassim, and S.H. Wei, *Electronic, energetic and chemical effects of intrinsic defects and Fe-doping of $CoAl_2O_4$: a DFT + U study*, J. Phys. Chem. C 112 (2008), pp. 12044–12050.

[24] M. Nolan and G.W. Watson, *Hole localization in Al doped silica: a DFT + U description*, J. Chem. Phys. 125 (2006), 144701.

[25] D.O. Scanlon, A. Walsh, B.J. Morgan, M. Nolan, J. Fearon, and G.W. Watson, *Surface sensitivity in lithium-doping of MgO: a density functional theory study with correction for on-site Coulomb interactions*, J. Phys. Chem. C 111 (2007), pp. 7971–7979.

[26] L.A. Curtiss, K. Raghavachari, P.C. Redfern, and J.A. Pople, *Assessment of Gaussian-2 and density functional theories for the computation of enthalpies of formation*, J. Chem. Phys. 106 (1997), pp. 1063–1079.

[27] A. Momma and F. Izumi, *VESTA: a three dimensional visualization system for electronic and structural analysis*, J. Appl. Cryst. 41 (2008), pp. 653–658.

[28] M. Nolan, S.C. Parker, and G.W. Watson, *CeO_2 catalysed conversion of CO, NO_2 and NO from first principles energetics*, Phys. Chem. Chem. Phys. 8 (2006), pp. 216–218.

[29] R.F.W. Bader, *Atoms in Molecules – A Quantum Theory*, Oxford University Press, New York, 1990.